



ChemComm

'Click' conjugated porous polymer nanofilm with a large domain size created by a liquid/liquid interfacial protocol

Journal:	<i>ChemComm</i>
Manuscript ID	CC-COM-01-2020-000360.R1
Article Type:	Communication

SCHOLARONE™
Manuscripts

COMMUNICATION

‘Click’ conjugated porous polymer nanofilm with a large domain size created by a liquid/liquid interfacial protocol

Received 00th January 20xx,
Accepted 00th January 20xx

Joe Komeda,^a Ryo Shiotsuki,^a Amalia Rapakousiou,^b Ryota Sakamoto,^{*c} Ryojun Toyoda,^a Kazuyuki Iwase,^d Masaki Tsuji,^e Kazuhide Kamiya^{d,e} and Hiroshi Nishihara^a

DOI: 10.1039/x0xx00000x

A liquid/liquid interfacial method is used to synthesize a conjugated porous polymer nanofilm with a large domain size. Copper-catalyzed azide–alkyne cycloaddition between a triangular terminal alkyne and azide monomers at a water/dichloromethane interface generates a 1,2,3-triazole-linked polymer nanofilm featuring a large aspect ratio and robustness against heat and pH.

Two-dimensional (2D) polymeric materials have received considerable interest, and research has focused on inorganic materials such as graphene¹ and transition-metal dichalcogenides,² which are obtained by exfoliating bulk layered crystals. The promise of inorganic 2D materials has also stimulated research on molecule-based 2D materials over the last 15 years.³ Our group has reported metal–organic nanosheets synthesized by gas/liquid or liquid/liquid interfacial methods.⁴ Organic ligand molecules with two or more connecting points in organic solvent and metal ions in water were layered, so that reversible coordination bond formation occurred at the gas/liquid or liquid/liquid interface. The resultant nanofilms had nanometre thicknesses, but only reached lateral domain sizes on the order of micrometres to centimetres, depending on the nanosheet composition. We have also performed gas/liquid or liquid/liquid interfacial synthesis of covalent organic nanosheets based on irreversible

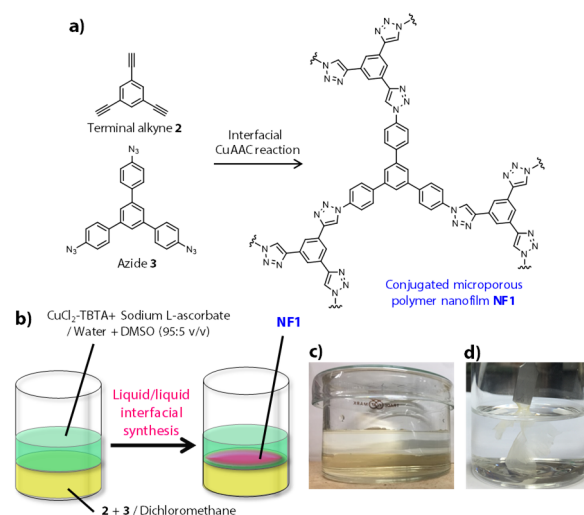


Fig. 1. (a) Synthetic scheme for “click” nanofilm **NF1**. (b) Schematic illustration of the liquid/liquid interfacial synthesis of **NF1**. (c) Photograph of the liquid/liquid interfacial reaction holding **NF1**. (d) **NF1** domains suspended in acetone, where **NF1** was picked up using a tweezer.

carbon–carbon bond formation.⁵ For example, graphdiyne was tethered precisely with the corresponding monomer, hexaethynylbenzene, through multiple alkyne–alkyne dimerization.^{5a} Another important class of molecule-based 2D materials is conjugated microporous polymer nanofilms (CMP-NFs).^{6,7} The strategy for creating CMPs is to use heavily cross-linked polymer motifs; however, the low solubility of such motifs often hampers the fabrication of films and membranes, and instead favours the formation of powdery particles. To overcome this problem, Livingston and coworkers accomplished a support-assisted liquid/liquid interfacial synthesis of CMP-NFs between carboxylic acyl chlorides and phenols/amines.^{6a,b} Jiang and coworkers conducted electropolymerization of triangular redox-active monomers to form several polymer films.^{6c,d} Tsotsalas and coworkers used a metal–organic framework thin film as a removable scaffold, on which a CMP-NF was grown by copper-catalyzed azide–alkyne cycloaddition (CuAAC)⁸ via a layer-by-layer technique.^{6e,f} In the

^a Department of Chemistry, Graduate School of Science, The University of Tokyo, 7-3-1, Hongo, Bunkyo-ku, Tokyo 113-0033, Japan

^b Laboratoire de Chimie de Coordination du CNRS, 205, Route de Narbonne, BP 44099, 31077, Toulouse, CEDEX 04, France

^c Department of Energy and Hydrocarbon Chemistry, Graduate School of Engineering, Kyoto University, Nishikyo-ku, Kyoto 615-8510, Japan

^d Research Center for Solar Energy Chemistry, Osaka University, 1-3 Machikaneyama, Toyonaka, Osaka 560-8531, Japan

^e Graduate School of Engineering Science, Osaka University, 1-3 Machikaneyama, Toyonaka, Osaka 560-8531, Japan

†Electronic Supplementary Information (ESI) available: Experimental details, Time-course **NF1** growth, dependence of the diameter of **NF1** on the size of the reaction container, relationship between the thickness of **NF1** and reaction time, height histogram for **NF1**, adsorption/desorption isotherms for **NF1** with N₂, H₂O, and CO₂ gases and BET surface evaluation, XPS of **NF1** after immersion in acidic and basic aqueous solutions, out-of-plane proton conductivity for **NF1**, XPS for **Pt@NF1**, and synthesis of another click nanofilm **NF4**. See DOI: 10.1039/x0xx00000x

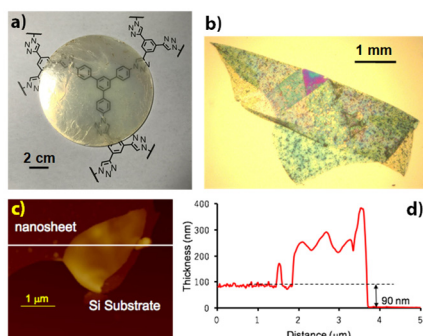


Fig. 2. Macroscopic and microscopic observations for **NF1**. (a) Photograph on a glass substrate with a diameter of 12 cm. (b) Optical microscopic image on a glass substrate. (c) AFM height image on a HMDS-modified $\text{SiO}_2/\text{Si}(111)$ substrate. (d) AFM cross-sectional profile along the white line in (c).

present paper, we describe the bottom-up, liquid/liquid interfacial synthesis of a click CMP-NF (**NF1**, Fig. 1a). We previously reported a prototype of the click CMP-NF, although its domain size was only 50 μm .⁹ In contrast, the modified liquid/liquid interfacial protocol we report here produced free-standing **NF1** with a large domain size 12 cm in diameter. We characterize and obtain macro- and microscopic observations of the vast domain, and we measure the porosity, chemical, and thermal durability, and metal and dye molecule uptake of **NF1**.

The synthetic scheme and chemical composition of the click CMP-NF, **NF1**, are shown in Fig. 1a. **NF1** comprises commercially available 1,3,5-triethynylbenzene (**2**) and 1,3,5-tris(4-azidophenyl)benzene¹⁰ (**3**). The liquid/liquid interfacial synthesis allowed the starting monomer materials to react with each other and form a film with a large domain size (Fig. 1b). The hydrophobic lower phase consisted of dichloromethane containing equimolar amounts of three-way terminal alkyne **2** and azide **3**. The hydrophilic upper phase comprised a mixture of water and DMSO (19:1 v/v) containing sodium L-ascorbate and a complex of copper(II) chloride and tris[(1-benzyl-1*H*-1,2,3-triazol-4-yl)methyl]amine ($\text{CuCl}_2\text{-TBTA}$).^{11b} The Cu^{2+} ions were reduced in situ by sodium L-ascorbate to Cu^+ , which is the catalyst for CuAAC.⁸ TBTA is a co-catalyst that accelerates CuAAC.¹¹ The biphasic reaction system was left to stand at room temperature for 48 h, during which time an **NF1** film was

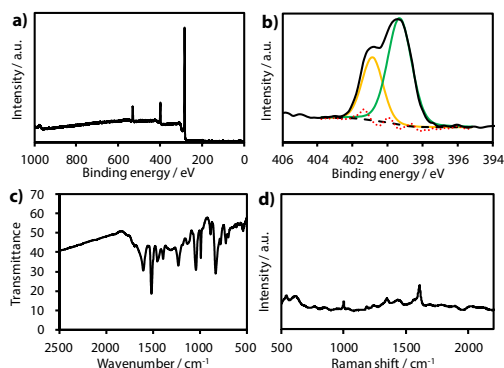


Fig. 3. (a,b) XPS for **NF1** on a $\text{SiO}_2/\text{Si}(111)$ substrate: (a) survey scan and (b) narrow scan focusing on the N 1s region. Black solid: experimental; yellow and green: fitting Gaussian functions; black dashed: background; red dotted: residual error. (c) IR spectra of **NF1** as a KBr pellet. (d) Raman spectrum of **NF1** on a copper substrate.

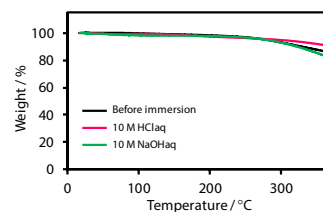


Fig. 4. TGA charts for **NF1** before and after the immersion in aqueous 10 M HCl or 10 M NaOH for 10 d at room temperature.

formed (Fig. 1c). Time-course growth of **NF1** indicated that at least 13.5 h was required to cover the whole liquid/liquid interface (Fig. S1[†]). The **NF1** film was rinsed with dichloromethane, aqueous HCl, water, and acetone to remove reaction residues and the copper catalyst. The **NF1** film was sufficiently robust, insoluble, and free-standing to pick up with tweezers (Fig. 1d). A typical yield of **NF1** was 27%.

An advantage of the liquid/liquid interfacial synthesis shown in Fig. 1b is that the domain size of the nanofilm can be tuned by choosing the size of the reaction container. We synthesized a single-domain **NF1** film with a diameter of 12 cm, which could be transferred onto any substrate, such as a glass plate, without introducing visible defects (Fig. 2a). In a similar manner, 7- and 4-cm-diameter **NF1** films were also fabricated (Fig. S2[†]). This series of results is attractive for producing membrane materials. The liquid/liquid interfacial reaction without TBTA produced a small domain only 20 μm in size.⁸ The morphology of **NF1** was examined by several microscopic techniques. An optical microscopic image of **NF1** showed a sheet morphology with a folded structure (Fig. 2b). Atomic force microscopy (Fig. 2c) showed an **NF1** domain partially folded over, again indicating that it was a sheet. The AFM cross-sectional profile showed that the folded region was rippled, whereas the intact **NF1** domain had a flat height profile (Fig. 2d). The thickness of **NF1** could be controlled by the reaction time (Fig. S3[†]). Fig. S4[†] assembled an AFM height histogram for a sheet of **NF1**, indicative of its flat surface. The average thickness of **NF1** was 93 ± 5 nm.

NF1 was characterized by various spectroscopic techniques. Fig. 3a shows an X-ray photoelectron spectroscopy (XPS) survey scan for **NF1** on a $\text{SiO}_2/\text{Si}(111)$ substrate, which identified constitutive nitrogen and confirmed that no copper catalyst peak was present around 930 eV. Fig. 3b shows a narrow scan for the N 1s region, featuring a double peak that was deconvoluted into two Gaussian functions centered at 399.4 and 400.8 eV. Based on the binding energy, the two peaks were

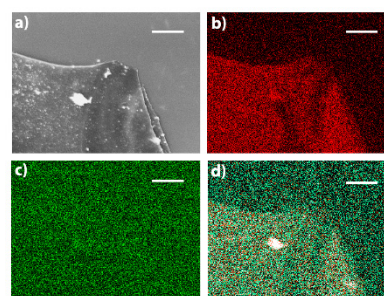


Fig. 5. (a) SEM image of **Pt@NF1** on a $\text{SiO}_2/\text{Si}(111)$ substrate. (b-d) SEM/EDS images of **Pt@NF1** for (b) carbon; (c) copper; and (d) platinum. Scale bar: 1 μm .

assigned to -N=N=N- and -N=N=N- chemical species in the 1,2,3-triazolyl group, respectively.¹² The two Gaussian functions had an area ratio of 2:1, consistent with the abundance of the nitrogen species in the triazole group. Azides tend to appear at around 404 eV;¹³ however, **NF1** did not show a peak in this region, indicating that there were no azides derived from **3**. The infrared (IR) spectrum for **NF1** showed typical absorption bands for 1,2,3-triazole, at 1239 cm^{-1} (C–N) and 1400–1800 cm^{-1} (N=N and C=C) (Fig. 3c).¹⁴ However, there were no peaks at around 2100 cm^{-1} derived from the monomers (C \equiv C and N₃).⁸ The Raman spectrum was consistent with the IR spectrum (Fig. 3d); there were no signals derived from C \equiv C and N₃ groups at around 2100 cm^{-1} , whereas there were bands at around 600 nm and 1100–1600 cm^{-1} originating from the 1,2,3-triazolyl group.¹⁵ The spectroscopic analysis indicated the quantitative generation of the 1,2,3-triazolyl linkage in **NF1**, with negligible residual terminal alkyne and azide residues. The porous structure of **NF1** was confirmed by N₂, water, and CO₂ adsorption/desorption, and the Brunauer–Emmett–Teller surface area was 110 $\text{m}^2 \text{g}^{-1}$ for N₂ (Fig. S5[†]).

Chemical stability was determined by immersing **NF1** in aqueous 10 M HCl or 10 M NaOH for 10 day at room temperature. After immersion, the N 1s peak in XPS had not change substantially, and was deconvoluted in the same way (Fig. S6[†]) as before immersion (Fig. 3b). Furthermore, before and after immersion, **NF1** was subjected to thermogravimetric analysis (TGA). It showed good thermal durability up to 300 °C, and negligible changes after immersion (Fig. 4). Thus, **NF1** showed good chemical and thermal stability.

The porous structure of **NF1** was examined in three experiments. The out-of-plane proton conductivity of **NF1** was tested using the set-up shown in Fig. S7a[†]; however, the conductivity was low despite the basicity of the triazolyl groups¹⁶ (Fig. S7b,c[†]). Next, the coordinating ability of triazole¹⁶ was tested in the uptake of platinum. **NF1** was immersed in an aqueous solution of K₂PtCl₄, and the conjugate was reduced in aqueous NaBH₄ to obtain Pt@**NF1**. Fig. 5a shows a scanning electron microscopy (SEM) image of Pt@**NF1**, and Fig. 5b–d show SEM/electron dispersive X-ray spectroscopy (EDS) images. The images showed the presence of Pt and the absence of Cu. Nitrogen was not observed by SEM/EDS because of the low sensitivity of the technique; however, its presence was confirmed by XPS, as well as by the coordination of Pt (Fig. S8[†]).

Fig. S9[†] represents a preliminary result for another click CMP-NF, **NF4**, which employed a different azide monomer. In this case the liquid/liquid interfacial protocol realized the formation of a nanofilm.

In conclusion, we performed a liquid/liquid interfacial synthesis of CMP-NF. Three-way terminal alkyne **2** and azide **3** were tethered using an interfacial click CuAAC reaction, forming free-standing CMP-NF **NF1**. The addition of TBTA allowed the formation of a large-domain nanofilm with a large aspect ratio, with a lateral size of up to 12 cm but a thickness of only 90 nm. Spectroscopic analysis confirmed the formation of the 1,2,3-triazolyl group and the absence of the ethynyl and azide residues from the monomers. **NF1** resisted hydrolysis under harsh conditions in concentrated acidic and basic aqueous

solutions, and also showed thermal stability up to 300 °C. Its porosity was investigated by gas adsorption/desorption experiments and by the uptake of platinum and Rhodamine B. The present work offers a new strategy for fabricating functional 2D porous polymeric nanofilms with large domain sizes.

The present work was chiefly supported by JST-CREST “Innovative reactions” to R.S. (JPMJCR18R3). The authors also acknowledge Grants-in-Aid from MEXT of Japan (Nos. 19H04562, 19H05377, 18K19094, 17H03028, 19H05460, 26220801, areas 2802 [Coordination Asymmetry]) and 8006 [Molecular Engine], and JST-CREST (JPMJCR15F2). R.S. is grateful to SEI Group CSR Foundation, NISSANKEN, Tobe Maki Scholarship Foundation, JGC-S Scholarship Foundation, Takahashi Industrial and Economic Research Foundation, Nippon Sheet Glass Foundation for Materials Science and Engineering, Tokyo Chemical Industry Foundation, Kondo Memorial Foundation, and The Asahi Glass Foundation for financial supports.

Conflicts of interest

There are no conflicts to declare.

Notes and references

- 1 A. K. Geim, *Science*, 2009, **324**, 1530.
- 2 C. Tan and H. Zhang, *Chem. Soc. Rev.*, 2015, **44**, 2713.
- 3 (a) D. Rodriguez-San-Miguel, P. Amo-Ochoa and F. Zamora, *Chem. Commun.*, 2016, **52**, 4113; (b) S.-L. Cai, W.-G. Zhang, R. N. Zuckermann, Z.-T. Li, X. Zhao and Y. Liu, *Adv. Mater.*, 2015, **27**, 5762; (c) J. W. Colson and W. R. Dichtel, *Nat. Chem.*, 2013, **5**, 453; (d) X. Feng and A. D. Schlüter, *Angew. Chem. Int. Ed.*, 2018, **57**, 13748; (e) R. Sakamoto, K. Takada, T. Pal, H. Maeda, T. Kambe and H. Nishihara, *Chem. Commun.*, 2017, **53**, 5781.
- 4 (a) T. Kambe, R. Sakamoto, K. Hoshiko, K. Takada, J. Ryu, S. Sasaki, J. Kim, K. Nakazato, M. Takata and H. Nishihara, *J. Am. Chem. Soc.*, 2013, **135**, 2462; (b) T. Kambe, R. Sakamoto, T. Kusamoto, T. Pal, N. Fukui, K. Hoshiko, T. Shimojima, Z. Wang, T. Hirahara, K. Ishizaka, S. Hasegawa, F. Liu and H. Nishihara, *J. Am. Chem. Soc.*, 2014, **136**, 14357; (c) R. Sakamoto, K. Hoshiko, Q. Liu, T. Yagi, T. Nagayama, S. Kusaka, M. Tsuchiya, Y. Kitagawa, W.-Y. Wong and H. Nishihara, *Nat. Commun.*, 2015, **6**, 6713; (d) K. Takada, R. Sakamoto, S.-T. Yi, S. Katagiri, T. Kambe and H. Nishihara, *J. Am. Chem. Soc.*, 2015, **137**, 4681; (e) R. Sakamoto, T. Yagi, K. Hoshiko, S. Kusaka, R. Matsuoka, H. Maeda, Z. Liu, Q. Liu, W.-Y. Wong and H. Nishihara, *Angew. Chem. Int. Ed.*, 2017, **56**, 3526; (f) T. Tsukamoto, K. Takada, R. Sakamoto, R. Matsuoka, R. Toyoda, H. Maeda, T. Yagi, M. Nishikawa, N. Shinjo, S. Amano, T. Iokawa, N. Ishibashi, T. Oi, K. Kanayama, R. Kinugawa, Y. Koda, T. Komura, S. Nakajima, R. Fukuyama, N. Fuse, M. Mizui, M. Miyasaki, Y. Yamashita, K. Yamada, W. Zhang, R. Han, W. Liu, T. Tsubomura and H. Nishihara, *J. Am. Chem. Soc.*, 2017, **139**, 5359; (g) X. Sun, K.-H. Wu, R. Sakamoto, T. Kusamoto, H. Maeda, X. Ni, W. Jiang, F. Liu, S. Sasaki, H. Masunaga and H. Nishihara, *Chem. Sci.*, 2017, **8**, 8078.
- 5 (a) R. Matsuoka, R. Sakamoto, K. Hoshiko, S. Sasaki, H. Masunaga, K. Nagashio and H. Nishihara, *J. Am. Chem. Soc.*, 2017, **139**, 3145; (b) R. Matsuoka, R. Toyoda, R. Shiotsuki, N. Fukui, K. Wada, H. Maeda, R. Sakamoto, S. Sasaki, H. Masunaga, K. Nagashio and H. Nishihara, *ACS Appl. Mater.*

- Interfaces*, 2019, **11**, 2730; (c) R. Sakamoto, R. Shiotsuki, K. Wada, N. Fukui, H. Maeda, J. Komeda, R. Sekine, K. Harano and H. Nishihara, *J. Mater. Chem. A*, 2018, **6**, 22189; (d) R. Sakamoto, N. Fukui, H. Maeda, R. Matsuoka, R. Toyoda and H. Nishihara, *Adv. Mater.*, 2019, **31**, 1804211.
- 6 (a) M. F. Jimenez-Solomon, Q. Song, K. E. Jelfs, M. Munoz-Ibanez and A. G. Livingston, *Nat. Mater.*, 2016, **15**, 760; (b) S. Karan, Z. Jiang and A. G. Livingston, *Science*, 2015, **348**, 1347; (c) C. Gu, N. Huang, Y. Chen, L. Qin, H. Xu, S. Zhang, F. Li, Y. Ma, D. Jiang, *Angew. Chem., Int. Ed.*, 2015, **54**, 13594; (d) C. Gu, N. Huang, J. Gao, F. Xu, Y. Xu and D. Jiang, *Angew. Chem., Int. Ed.*, 2014, **53**, 4850; (e) P. Lindemann, A. Schade, L. Monnereau, W. Feng, K. Batra, H. Gliemann, P. Levkin, S. Bräse, C. Wöll and M. Tsotsalas, *J. Mater. Chem. A*, 2016, **4**, 6815. (f) P. Lindemann, M. Tsotsalas, S. Shishatskiy, V. Abetz, P. Krolla-Sidenstein, C. Azucena, L. Monnereau, A. Beyer, A. Götzhäuser, V. Mugnaini, H. Gliemann, S. Bräse and C. Wöll, *Chem. Mater.*, 2014, **26**, 7189.
- 7 (a) N. Chaoui, M. Trunk, R. Dawson, J. Schmidt and A. Thomas, *Chem. Soc. Rev.*, 2017, **46**, 3302; (b) G. Cheng, B. Bonillo, R. S. Sprick, D. J. Adams, T. Hasell and A. I. Cooper, *Adv. Funct. Mater.*, 2014, **24**, 5219; (c) C. Gu, Y. Chen, Z. Zhang, S. Xue, S. Sun, K. Zhang, C. Zhong, H. Zhang, Y. Pan, Y. Lv, Y. Yang, F. Li, S. Zhang, F. Huang and Y. Ma, *Adv. Mater.*, 2013, **25**, 3443; (d) W.-E. Lee, Y.-J. Jin, L.-S. Park and G. Kwak, *Adv. Mater.*, 2012, **24**, 5604; (e) K. Yuan, X. Zhuang, H. Fu, G. Brunklau, M. Forster, Y. Chen, X. Feng and U. Scherf, *Angew. Chem., Int. Ed.*, 2016, **55**, 6858; (f) X. Zhuang, D. Gehrig, N. Forler, H. Liang, M. Wagner, M. R. Hansen, F. Laquai, F. Zhang and X. Feng, *Adv. Mater.*, 2015, **27**, 3789; (g) P. Pandey, O. K. Farha, A. M. Spokoyny, C. A. Mirkin, M. G. Kanatzidis, J. T. Hupp and S. T. Nguyen, *J. Mater. Chem.*, 2011, **21**, 1700.
- 8 (a) M. Meldal and C. W. Tornøe, *Chem. Rev.*, 2008, **108**, 2952; (b) J. E. Heina and V. V. Fokin, *Chem. Soc. Rev.*, 2010, **39**, 1302; (c) C. Wang, D. Ikhlef, S. Kahlal, J.-Y. Saillard and D. Astruc, *Coord. Chem. Rev.*, 2016, **316**, 1.
- 9 A. Rapakousiou, R. Sakamoto, R. Shiotsuki, R. Matsuoka, U. Nakajima, T. Pal, R. Shimada, A. Hossain, H. Masunaga, S. Horike, Y. Kitagawa, S. Sasaki, K. Kato, T. Ozawa, D. Astruc and H. Nishihara, *Chem. Eur. J.*, 2017, **23**, 8443.
- 10 (a) S. Kotha, D. Kashinath, K. Lahiri and R. B. Sunoj, *Eur. J. Org. Chem.*, 2004, **19**, 4003; (b) N. Oda, T. Nakai, K. Sato, D. Shiomi, M. Kozaki, K. Okada and T. Takui, *Mol. Cryst. Liq. Cryst.*, 2002, **376**, 501; (c) W. Zhu and D. Ma, *Chem. Commun.*, 2004, 888.
- 11 (a) T. R. Chan, R. Hilgraf, K. B. Sharpless and V. V. Fokin, *Org. Lett.*, 2004, **6**, 2853; (b) P. S. Donnelly, S. D. Zanatta, S. C. Zammit, J. M. White and S. J. Williams, *Chem. Commun.*, 2008, 2459.
- 12 (a) X. Liu, H.-N. Zheng, Y.-Z. Ma, Q. Yan and S.-J. Xiao, *J. Colloid Interface Sci.*, 2011, **358**, 116. (b) S. Ciampi, T. Böcking, K. A. Kilian, M. James, J. B. Harper and J. J. Gooding, *Langmuir*, 2007, **23**, 9320.
- 13 (a) P. Cao, K. Xu and J. R. Heath, *J. Am. Chem. Soc.*, 2008, **130**, 14910; (b) A. E. Dugaard and S. Hvilsted, *Macromolecules*, 2008, **41**, 4321.
- 14 S. Sun and P. Wu, *J. Phys. Chem. A*, 2010, **114**, 8331; (b) A. Rapakousiou, Y. Wang, C. Belin, N. Pinaud, J. Ruiz and D. Astruc, *Inorg. Chem.*, 2013, **52**, 6685.
- 15 B. K. Yoo and S.-W. Joo, *J. Colloid Interface Sci.*, 2007, **311**, 491.
- 16 D. Huang, P. Zhao and D. Astruc, *Coord. Chem. Rev.* 2014, **272**, 145.

Synopsis: Copper-catalyzed azide–alkyne cycloaddition between a triangular terminal alkyne and azide monomers at a water/dichloromethane interface generates a 1,2,3-triazole-linked polymer nanofilm with a large aspect ratio, a lateral dimension of 12 cm, and thickness of 90 nm. The robust hyper-cross-linked triazole linkage allows the nanofilm to resist hydrolysis under harsh acidic and alkaline conditions, and to resist pyrolysis up to 300 °C.

